Regulatory Toxicology and Pharmacology 72 (2015) 447–457

Contents lists available at ScienceDirect

Regulatory Toxicology and Pharmacology

journal homepage: www.elsevier.com/locate/yrtph

Bioaccessibility of micron-sized powder particles of molybdenum metal, iron metal, molybdenum oxides and ferromolybdenum – Importance of surface oxides

Alexander Mörsdorf, Inger Odnevall Wallinder, Yolanda Hedberg *

KTH Royal Institute of Technology, School of Chemical Science and Engineering, Department of Chemistry, Division of Surface and Corrosion Science, Drottning Kristinas väg 51, SE-10044 Stockholm, Sweden

ARTICLE INFO

Article history:
Received 2 March 2015
Available online 29 May 2015

Keywords:
Molybdenum
Ferromolybdenum
Alloy
Bioaccessibility
Surface oxide

ABSTRACT

The European chemical framework REACH requires that hazards and risks posed by chemicals, including alloys and metals, that are manufactured, imported or used in different products (substances or articles) are identified and proven safe for humans and the environment. Metals and alloys need hence to be investigated on their extent of released metals (bioaccessibility) in biologically relevant environments. Read-across from available studies may be used for similar materials. This study investigates the release of molybdenum and iron from powder particles of molybdenum metal (Mo), a ferromolybdenum alloy (FeMo), an iron metal powder (Fe), MoO_2, and MoO_3 in different synthetic body fluids of pH ranging from 1.5 to 7.4 and of different composition. Spectroscopic tools and cyclic voltammetry have been employed to characterize surface oxides, microscopy, light scattering and nitrogen absorption for particle characterization, and atomic absorption spectroscopy to quantify released amounts of metals. The release of molybdenum from the Mo powder generally increased with pH and was influenced by the fluid composition. The mixed iron and molybdenum surface oxide of the FeMo powder acted as a barrier both at acidic and weakly alkaline conditions. These findings underline the importance of the surface oxide characteristics for the bioaccessibility of metal alloys.

1. Introduction

REACH (Registration, Evaluation, Authorisation and Restriction of Chemicals) is a European Chemicals Directive first implemented in July 2007. Its aim is to evaluate, document and restrict the application and progression of chemicals manufactured and processed in the European Union in quantities that exceed 1 tonne per company and year (EC, 2007). Within REACH, metals are considered as substances for which registration dossiers have to be submitted. Such dossiers include the assessment of the toxicological and ecotoxicological hazard profile, for which the specific bioaccessibility in biological fluids plays an important role. Bioaccessibility is here defined as the pool of released metals from a metal or alloy that potentially can become available for absorption by an organism and is measured as the total amount of released metal species in solution after separation from the powder particles. The bioavailable fraction of released metal species in solution may be significantly lower compared with the total concentration. However, this was not studied within the scope of this paper.

Alloys are generally considered as special mixtures under REACH, for which no registration dossiers need to be prepared. So far, very few alloys on the market have been investigated individually. An alloy is as *"a metallic material, homogeneous on a macroscopic scale, consisting of two or more elements so combined that they cannot be readily separated by mechanical means"* (EC, 2009). An alloy is hence totally different from a chemical mixture. One or several elements are intentionally added to the base element, which constitutes the largest percentage of the material, to gain specific mechanical or physico-chemical properties compared with its pure alloy components. These changes in intrinsic properties make any translation, such as metal release rates of individual elements to an alloy of the same elements inaccurate and irrelevant. As a result, properties of alloys are in need of evaluation based on its alloy specific characteristics, and not on its pure constituent metals. Potential health risks of alloys have in some cases been estimated via read-across from the properties of the respective pure metals. However recent studies show that the surface properties of alloys are more important than their bulk

* Corresponding author. Fax: +46 8 208284.
E-mail address: yolanda@kth.se (Y. Hedberg).

http://dx.doi.org/10.1016/j.yrtph.2015.05.027
0273-2300/

composition, and that read-across from pure metals is often highly erroneous (Hedberg et al., 2013; Herting et al., 2005; Hillwalker and Anderson, 2014; Stockmann-Juvala et al., 2013).

Metal release from metals and alloys, without contribution of wear, is mainly governed by oxidation of the metal (corrosion) and of chemical dissolution of the surface oxide. These processes depend on the passive properties of the surface oxide (hinders corrosion) and, among others, the pH and metal complexation capacity of the surrounding fluid (Hedberg et al., 2011b; Hedberg and Midander, 2014; Mazinanian et al., 2015). Available corrosion and metal release studies in the literature on molybdenum-containing alloys are mainly focused on alloys (and metals) commonly used in technical or medical applications (*e.g.* corrosion-resistant stainless steel or implants) (Cobb and Schmalzreid, 2006; Hanawa, 2004; Hedberg and Odnevall Wallinder, 2014; Hedberg et al., 2014; Hillwalker and Anderson, 2014; Ichinose et al., 2003; Karimi et al., 2012; Lewis et al., 2005; Metikoš-Huković et al., 2006; Okazaki and Gotoh, 2005, 2008; Öztürk et al., 2006; Wataha, 2000). However, metal release data from molybdenum-containing biomedical implants may not necessarily follow similar trends as observed for pure molybdenum metal or ferromolybdenum alloys, as the corrosion properties of these materials are largely different (Hodgson et al., 2004; Kocijan et al., 2004). Mechanistic metal release investigations of molybdenum metal, ferromolybdenum alloys, or molybdenum oxides are scarcely reported in the scientific literature, despite their increasing use in different applications during the last decades. Molybdenum or molybdenum oxide nanoparticles are for example used for bio-diagnostics and energy storage applications as well as in polymers (Chan et al., 2005; Lee et al., 2009; Sengupta et al., 2014). Molybdenum shows relatively low acute toxicity, when taken up via the oral, dermal or inhalation route (OECD CoCAM programme, 2013).

The aim of this study is to correlate particle characteristics and surface composition with the extent of metal release from micron-sized powder particles of molybdenum (Mo) metal, iron (Fe) metal, and a ferromolybdenum (FeMo) alloy into five synthetic body fluids of relevance for the human exposure routes of dermal contact, inhalation and ingestion. Parallel comparative studies were performed on MoO_2 and MoO_3 powder particles.

2. Materials and methods

2.1. Investigated particles

This investigation includes the following micron-sized powder particles; (i) molybdenum (Mo) metal (>99.95 wt%), CAS No. 7439-98-7, Batch No. C198, produced by CM CHEMIEMETALL GmbH, Bitterfeld, Germany, (ii) a ferromolybdenum (FeMo) alloy (Mo content 69.8 wt%), CAS No. 94277-04-0, Batch No. 1010/07/2, produced by Treibacher Industrie AG, Treibach-Althofen, Germany, (iii) iron metal (Fe, >99.8 wt%), CAS No. 7439-89-6, Batch No. 1946672, produced by Höganäs AB, Höganäs, Sweden, (iv) molybdenum(IV)oxide (MoO_2, >99.99 wt%), CAS No. 18868-43-4, Batch No. D1308 DRO, produced by CM CHEMIEMETALL GmbH, Bitterfeld, Germany, and (v) molybdenum(VI)oxide (MoO_3, >99.99 wt%), CAS No. 1313-27-5, Batch No. RTPOC0080G, produced by Climax Molybdenum Company, Rozenburg/Rotterdam, Netherlands.

2.2. Cyclic voltammetry using a graphite paste electrode

Each molybdenum-containing powder (Mo, FeMo, MoO_2, MoO_3) was mixed with graphite powder (natural, briquetting grade, 100 mesh, 99.9995% (metal basis), UCP-1 grade, Ultra "F" grade, Lot No. 61200620, Alfa Aesar, Sweden) in a ratio of 100 mg graphite and 1, 5, or 10 mg metal/alloy/oxide powder. This mixture was gently pressed and mixed with a pestle. A few drops of the electrolyte [8 M NaOH (pH 13.6), a solution of sodium acetate/acetic acid (0.1 M sodium acetate, 0.1 M acetic acid, pH 4.62), or 1 M HCl (pH 0)] were added to obtain a paste. The paste was positioned into a small (Ø 1.9 cm, height 7.0 cm) glass container connected with a platinum wire to act as the working electrode. The counter electrode (a platinum wire wrapped around the reference electrode) and the reference electrode (Ag/AgCl sat. KCl) were positioned approximately 1 cm from the graphite paste in the electrolyte. The system was, prior to the measurements, allowed to equilibrate before determining the open circuit potential (OCP) for 300 s (or until the change of OCP was less than 1 μV/s). The potential was then swept cathodically (to more negative potentials) starting at the OCP at a rate of 0.0005 V/s toward a potential of approximately −1.4 V (*vs.* Ag/AgCl sat. KCl), after which the potential was swept anodically until a potential of approximately +0.2 V.

2.3. Raman spectroscopy

Raman spectroscopy measurements were conducted using a Horiba HR800 Raman (Yvon Jobin) instrument using a 785 nm laser and an Olympus 50X objective. The laser power was attenuated to avoid sample damage. A visual inspection (optical microscope) was made prior to, and after each measurement, to ensure minimized sample destruction (via oxidation by the laser). In the case of visible sample destruction, the spectrum was not taken into account. Presented results are based on average spectra accumulated for 35 s at 3–5 different sample locations (MoO_2, FeMo), or one sample location (Mo, MoO_3 – no signal for Mo, very strong signal for MoO_3). No sufficient signal was obtained for the Fe powder, even with a 514 nm laser, a 100X objective, and an accumulation time of 60 s, and without any laser attenuation.

2.4. X-ray photoelectron spectroscopy

With X-ray photoelectron spectroscopy (XPS) using a Kratos AXIS UltraDLD X-ray photoelectron spectrometer (Kratos Analytical, Manchester, UK) driven by a monochromatic 150 W Al X-ray source, the outermost (approx. 5 nm) surface of the powder particles was investigated. The analyzed areas were approximately sized 700 × 300 μm. Wide spectra measurements were performed to probe elements in the top surface of the powder particles. With a pass energy of 20 eV, detailed spectra for the main compositional elements of each powder, carbon (C 1s), oxygen (O 1s), nitrogen (N 1s), iron (Fe 2p) and molybdenum (Mo 3d) were obtained. The powders were mounted on copper tape to fix them against diffusion in the applied vacuum inside the ultra-high vacuum instrumental chamber. All binding energies were corrected to the carbon C 1s contamination peak at 285.0 eV. All peak areas were determined by assigning a linear base line. For the calculation of atomic ratios of oxidized metal and oxygen, the metal peak (only detected for Mo at 228.4 ± 0.4 eV) was subtracted. Oxygen connected to any oxidized carbon compounds from the ambient air was not subtracted, however, its contribution was considered small due to the lack of (Mo-metal powder) or minor presence of oxidized carbon peaks (FeMo alloy, MoO_2, and MoO_3 powders).

2.5. Measurement of specific surface area by nitrogen adsorption

The surface area to weight ratio (specific surface area) of each powder was estimated using the Brunauer–Emmet–Teller method (Brunauer et al., 1938) (Micromeritics GEMINI V) that measures the adsorbed amount of nitrogen at cryogenic conditions. The

measurements were performed at five different partial pressures and at five different local positions for each powder (standard BET method). The standard deviation was less than 1% for the measurements.

2.6. Light scattering

The particle size distribution of each powder was determined in phosphate buffered saline (PBS, pH 7.4, see Section 2.8) using low angle laser light scattering (Malvern Mastersizer 2000, with a Hydro SM dispersion unit). Refractive indexes for molybdenum (3.71) and water (1.33, the solvent for the test media) for Mo, FeMo, MoO_2, and MoO_3 powders, and refractive indexes for iron (2.86) and water for the Fe powder were used as input parameters for the calculation of the size distribution by volume. Data is presented as average numbers with standard deviation of at least three discrete measurements of each powder.

The particle size distribution of each powder was furthermore determined at dry conditions for the Fe metal powder (CILAS 1090D, at an air stream pressure of 500 mbar) and the Mo, FeMo, MoO_2, and MoO_3 powders (Malvern Mastersizer MAM2461, air pressure 1500 mbar) using the Fraunhofer theory.

2.7. Scanning electron microscopy

Particle morphologies were studied using a tabletop scanning electron microscope (SEM) with backscattered electron analysis (Hitachi TM-1000). The powders were fixed on carbon tape to avoid dispersion inside the instrument chamber and to assure appropriate conduction.

2.8. Exposure to synthetic body fluids

Triplicate samples of each powder were exposed for 2 and 24 h to each of the five synthetic body fluids (Table 1) at a ratio of 5 ± 0.5 mg particles in 50 mL solution (0.1 g/L) in closed PMP Nalgene® jars positioned in a Stuart platform-rocker incubator (25 cycles/min of bi-linear shaking) at 37 ± 0.5 °C. Blank samples (without powders) were run in parallel for each powder, solution, and exposure time. Exposures of the MoO_3 powder were made at a higher loading (50 ± 1 mg in 50 mL solution), which theoretically can suppress the extent of released molybdenum due to effects of particle agglomeration and chemical equilibrium compared with lower loadings (Hedberg and Odnevall Wallinder, 2012; Midander et al., 2006). However, since the MoO_3 powder completely dissolved in some fluids and released most of its molybdenum content, compared with the other powders, the difference in loading is not considered to influence any comparison with the other powders of this study. After exposure, the test fluid was separated from the powder particles by centrifugation at 3000 r.p.m. (704 r.c.f.) for 10 min. The supernatant solution, free of particles, was acidified to a pH less than 2 (not needed in the case of artificial gastric fluid) with 65% ultrapure HNO_3 prior to solution analysis (a standard procedure for metal analysis and conservation of samples). All vessels for exposure, centrifugation and storage were acid-cleaned in 10% HNO_3 for at least 24 h, rinsed four times with ultra-pure water, and dried in ambient laboratory air to minimize the risk of contamination.

Five synthetic body fluids were selected:

- Phosphate-buffered saline (PBS, pH 7.2–7.4), a standard physiological fluid that mimics the ionic strength of human blood serum.
- Gamble's solution (GMB, pH 7.4), mimics the interstitial fluid within the deep lung under normal health conditions (Stopford et al., 2003).
- Artificial sweat (ASW, pH 6.5), simulates the hypoosmolar fluid, linked to hyponatraemia (loss of Na^+ from blood), which is excreted from the body upon sweating. The fluid is recommended in the available standard for testing of nickel release from nickel containing products (CEN, 2011).
- Artificial lysosomal fluid (ALF, pH 4.5), simulates intracellular conditions in lung cells occurring in conjunction with phagocytosis and represents relatively harsh conditions (de Meringo et al., 1994; Hillwalker and Anderson, 2014).
- Artificial gastric fluid (GST, pH 1.5), mimics the very harsh digestion setting of high acidity in the stomach (Hamel et al., 1998).

2.9. Atomic absorption spectroscopy and data presentation

Total concentrations of released molybdenum in solution were analyzed by atomic absorption spectroscopy (AAS) using a

Table 1
Composition (g/L), initial, and final pH of the five synthetic body fluids.

Chemical	GST	ALF	ASW	PBS	GMB
$MgCl_2$	–	0.050	–	–	0.095
NaCl	–	3.21	5.0	8.77	6.02
KCl	–	–	–	–	0.298
Na_2HPO_4	–	0.071	–	1.28	0.126
KH_2PO_4	–	–	–	1.36	–
Na_2SO_4	–	0.039	–	–	0.063
$CaCl_2{\cdot}2H_2O$	–	0.128	–	–	0.368
$C_2H_3O_2Na{\cdot}H_2O$ (sodium acetate)	–	–	–	–	0.700
$NaHCO_3$	–	–	–	–	2.60
$C_6H_5Na_3O_7{\cdot}2H_2O$ (sodium citrate)	–	0.077	–	–	0.097
NaOH	–	6.00	–	–	–
Citric acid	–	20.8	–	–	–
Glycine	–	0.059	–	–	–
$C_4H_4O_6Na_2{\cdot}2H_2O$ (Na_2Tartrate$\cdot 2H_2O$)	–	0.090	–	–	–
$C_3H_5NaO_3$ (NaLactate)	–	0.085	–	–	–
$C_3H_5O_3Na$ (NaPyruvate)	–	0.086	–	–	–
$CH_3CHOHCO_2H$ (lactic acid)	–	–	1.0	–	–
$(NH_2)_2CO$ (urea)	–	–	1.0	–	–
HCl (25%)	4.0	–	–	–	–
Initial pH (prior to exposure)	1.7–1.8	4.5	6.4–6.6	7.2–7.3	7.3–7.4
Final pH (after exposure) – Mo, Fe, and FeMo	1.5–1.8	4.4–4.5	5.6–6.5	7.2–7.4	7.6–8.4
Final pH (after exposure) – MoO_2 and MoO_3	1.5–1.6	4.4–4.5	3.2–6.2	5.7–7.3	6.6–8.7

GST – artificial gastric solution; ALF – artificial lysosomal fluid; ASW – artificial sweat; PBS – phosphate buffered saline; GMB – Gamble's solution.

N_2O/acetylene-flame (mg/L, ppm range) and graphite furnace (GF-AAS, μg/L, ppb range). Calibration standards with molybdenum concentrations of 40, 120 and 360 mg/L were prepared using 1% HNO_3 to mimic the acidic condition of acidified solution samples for analysis when using the reducing N_2O/acetylene flame. 0.5% $AlCl_3$ was added to both the standards and the samples for molybdenum analysis in order to avoid interferences. Quality controls (in 1% HNO_3) were performed every third sample to ensure accurate and reliable data. Two matrix modifiers, palladium- and magnesium nitrate and calibration standards with molybdenum concentrations of 10, 30, and 100 μg/L were used for the GF-AAS analysis. Since very stable complexes are formed in the graphite furnace, the cleanout temperature was set to 2500 °C, the time for atomization to 5 s, and the cleanout time to 7 s. Quality controls were performed every ninth sample. Calibration standards with iron concentrations of 1, 5, and 10 mg/L, or 10, 30, and 100 mg/L (if the sample concentration exceeded 10 mg/L) were used for the air/acetylene flame analysis of iron (FeMo and Fe powders). The limits of detection, calculated as average blank values plus 3 times the highest standard deviation of the blanks in each solution, were between 1.0 (in PBS) and 4.4 μg/L (in ALF) for molybdenum analyzed using the graphite furnace mode, between 51 (ALF) and 75 μg/L (GMB) for molybdenum analyzed in the flame mode, and between 53 (GST) and 121 (ALF) μg/L for iron analyzed in the flame mode. All reported values are based on concentrations that are significantly higher than their corresponding limits of detection. Iron released from the Fe metal powder was below the limit of detection for the PBS and GMB fluids (both pH 7.4) and similar to the limit of detection for the ASW fluid after 2 h of exposure (pH 6.5), indicated in Fig. 3.

Release data is presented as the measured release of molybdenum normalized to the particle content of molybdenum (wt%), or the measured release of iron normalized to the particle content of iron (wt%), as follows:

$$\frac{\text{Aqueous metal concentration}\left(\frac{g}{l}\right) * \text{Volume}(0.05\ \text{L})}{\text{Sample mass}(g) * x} * 100 \qquad (1)$$

With $x = 1$ (Mo and Fe metal powders), 0.698 (molybdenum content of the FeMo alloy powder), 0.302 (iron content of the FeMo alloy powder), 0.750 (molybdenum content of the MoO_2 powder), and 0.667 (molybdenum content of the MoO_3 powder).

3. Results

3.1. Particle and surface characterization

Measured specific surface areas, including surface pores, are compiled for each powder in Table 2. These areas increased according the following sequence: Fe < FeMo < Mo < MoO_2 < MoO_3. An increased specific surface area is normally correlated with reduced particle size (unless large contribution of surface pores). The size distribution cut-off values (by volume) in PBS and at dry conditions are also included in Table 2. The SEM investigation and dry size distribution measurements revealed particle sizes typically smaller than 10 μm for the Mo metal powder. However, their size in PBS appeared larger, most probably as a result of agglomeration in solution. The FeMo alloy powder revealed relatively large particles, sized around 100 μm based on SEM imaging, but also significantly smaller particles as reflected in the size distribution measurements in PBS, Table 2. The Fe metal powder showed a relatively narrow size distribution (both at dry conditions and in PBS, Table 2) with an average size of approximately 100 μm. As evident from SEM imaging, Fig. 1, the molybdenum oxide powders formed agglomerates both in solution and at dry conditions. The MoO_3 powder showed smaller particles sizes when immersed in PBS compared with dry conditions.

Table 2
BET specific surface area (m^2/g) of the different powders investigated (relative standard deviation <1%), and 10, 50, and 90 vol% cut-off values (μm) for each powder when immersed in PBS (relative standard deviation <10%), and at dry conditions (relative standard deviation <21%).

Powder		Mo	Fe	FeMo	MoO_2	MoO_3
BET(m^2/g)		0.225	0.032	0.109	1.18	2.97
Immersed in PBS	d0.1 (μm)	8.75	50.4	8.50	12.5	1.18
	d0.5 (μm)	23.9	110	72.2	216	129
	d0.9 (μm)	56.9	215	181	416	244
Dry	d0.1 (μm)	3.70	50.7	32.6	5.70	21.3
	d0.5 (μm)	8.40	96.6	98.9	229	195
	d0.9 (μm)	15.5	177	176	402	365

The surface or bulk oxides of the powder particles were investigated by means of Raman spectroscopy (sensitive to oxides, but not to metals), by XPS (approx. 5 nm surface sensitivity), and cyclic voltammetry (able to distinguish between different oxides). Raman spectroscopy confirmed the bulk oxide composition of MoO_2 and MoO_3 for the two oxide powders, respectively (Table 3). The surface oxide of the FeMo alloy powder did neither contain MoO_3 nor hematite (α-Fe_2O_3), but a mixed Fe(III)/Mo(VI)-oxide, possibly similar to ferrimolybdite ($Fe_2(MoO_4)_3{\cdot}n(H_2O)$) (Table 3).

Except for adventitious carbon present at the surface on all powders, the main elements of each powder were observed in the outer layer by means of XPS. Observed binding energies are compiled in Table 4. Particles of both the Mo and the FeMo powder revealed thin (a few nm) surface oxides, as evident from peaks assigned as metallic Mo, Table 4. Mo(VI), the most oxidized form of molybdenum, was observed at the outermost surface on powder particles of MoO_2, Mo, and FeMo. Oxidized iron in the outermost surface was observed for the FeMo and Fe powders.

Cyclic voltammetry using a graphite paste electrode was employed in 8 M NaOH (pH 13.6), and acetate buffer (pH 4.6) for all molybdenum-containing powders (for selected powders also in 1 M HCl, pH 0) in order to investigate possible solid/solid transformations (from one oxide to another) or their dissolution properties. One reduction peak was observed for FeMo powder particles in 8 M NaOH at approx. −1.2 V (Ag/AgCl) and two oxidation peaks at approx. −0.9 and −0.8 V, corresponding to trivalent iron oxide (Hedberg et al., 2012; Linhardt, 1998; Neugebauer et al., 1981). These observations were not reproducible. No peaks corresponding to any solid/solid transformation were observed for any of the other measurements, powders, or electrolytes. The dissolution potentials for the Mo metal powder were observed at −0.6 V (*vs.* Ag/AgCl sat. KCl) in 8 M NaOH and at 0 V in acetate buffer. Oxidative dissolution of the powders took place in the different solutions in the following order:

- 8 M NaOH: FeMo (−0.6 V) ≈ Mo (−0.6 V) > MoO_2 (0.1 V) > MoO_3 (none).
- Acetate buffer: FeMo (−0.2 V) > Mo (0 V) > MoO_2 (0.3 V) > MoO_3 (none).

Dissolution in 1 M HCl was only examined for the MoO_2 powder that dissolved at 0.25 V.

3.2. Metal release in synthetic biological fluids of varying pH and metal complexation capacity

Amounts of molybdenum in solution released from powder particles of Mo, FeMo, MoO_2 and MoO_3 exposed for 2 and 24 h in the different synthetic body fluids are presented in Fig. 2. The Mo and FeMo powders showed strongly reduced release rates with time

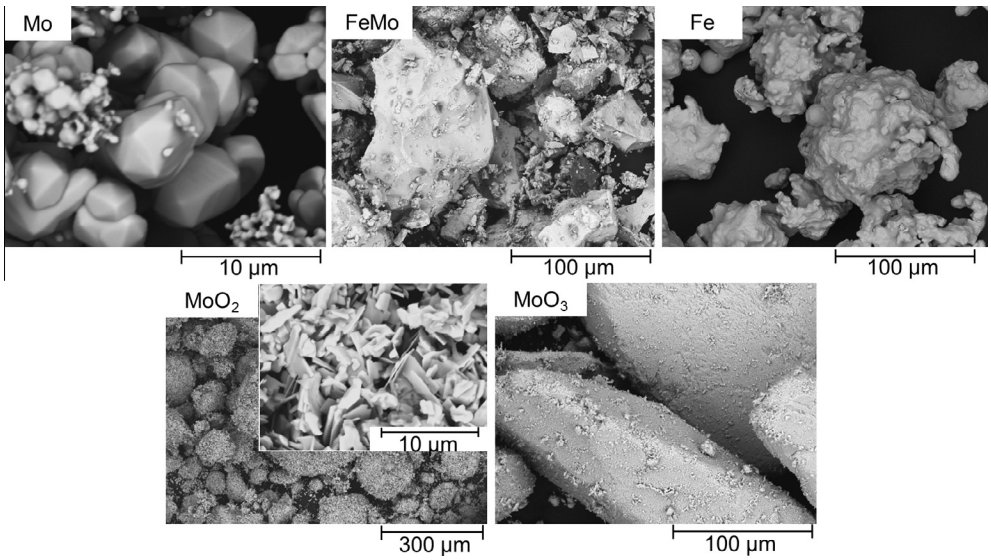

Fig. 1. SEM images of powder particles of Mo, FeMo, Fe, MoO_2 and MoO_3.

Table 3
Observed Raman bands (cm^{-1}) and their assignments for each powder. No information could be obtained for the Mo and Fe metal powders.

Powder	Observed Raman bands (cm^{-1})	Assignment (reference)
FeMo	218 s, 284 s, 350 w, 400 w, 600 w, 780–800 m br, 880 w, 923 vs	Possibly ferrimolybdite, $Fe_2(MoO_4)_3{\cdot}n(H_2O)$ (Kerr et al., 1963; Sejkora et al., 2014)
MoO_2	210 m, 229 m, 350 m, 363 s, 466 m, 490 m, 560 w, 580 w, 738 s	MoO_2 (Fleischer and Pabst, 1981; Kruglova et al., 1980; Kumari et al., 2007)
MoO_3	153 s, 240 m, 283 s, 340 m, 380 m, 670 m, 819 vs, 994 s	MoO_3 (Anthony et al., 1990; Kihlborg, 1963; Mestl et al., 1994; Solferino and Anderson, 2012)

vs – very strong, s – strong, m – moderate, w – weak, br – broad.

Table 4
Binding energies[a] (eV) of main peaks of Mo $3d_{5/2}$, O 1s and Fe $2p_{3/2}$ observed by means of XPS and their assignments.

	Mo $3d_{5/2}$	O 1s[b]	Fe $2p_{3/2}$	Assignment (reference)
Mo	228.6; 233.2	531.0	–	Mo metal (Werfel and Minni, 1983) Mo(VI) (Anwar et al., 1989; Colton et al., 1978)
Fe	–	530.7	711.9	Fe(ox) (Fujii et al., 1999; Grosvenor et al., 2004)
FeMo	228.0; 232.6	530.8	711.2	Mo metal (Werfel and Minni, 1983) Mo(VI) (Anwar et al., 1989; Colton et al., 1978) Fe(ox) (Fujii et al., 1999; Grosvenor et al., 2004)
MoO_2	229.9; 233.1	530.9	–	Mo(IV) (Colton et al., 1978) Mo(VI) (Anwar et al., 1989; Colton et al., 1978)
MoO_3	232.6	530.4	–	Mo(VI) (Anwar et al., 1989; Colton et al., 1978)

[a] Measurements from one surface area sized approximately 300 × 700 µm.
[b] The contribution of oxygen related to oxidized carbon constituents in the surface oxide was minor.

(amount of molybdenum released per time unit), especially in GST (pH 1.5) and GMB (pH 7.4). Reduced release rates with time were also observed for the MoO_2 powder. From Fig. 3, it can clearly be seen that the FeMo alloy powder did neither behave like the Fe metal powder nor like the Mo metal powder. The released amount of iron from the Fe metal powder was strongly pH-dependent with a high release into GST (pH 1.5) and non-detectable release into the neutral or weakly alkaline fluids of PBS and GMB (both pH 7.4). The release of molybdenum from the Mo powder showed the opposite pH-dependence (with the exception for the GMB fluid). Mo particles were dissolved up to 6% in PBS, up to 2% in ASW and less than 1% in GST, ALF and GMB. In contrast, the highest total amount of released metals in solution (Fe + Mo) was observed in ASW (pH 6.5) for the FeMo alloy powder. The corresponding release in the other fluids (GST, ALF, PBS and GMB) of both higher and lower solution pH was 4–20-fold lower, Fig. 3. Molybdenum (per molybdenum content in the FeMo powder) was dissolved up to 13% in ASW, about 2% in PBS and ALF, and less than 1% in GMB and GST. More iron compared with molybdenum was released at acidic conditions (GST), and more molybdenum compared with iron was released at higher pH values.

4. Discussion

4.1. Characterization of the powders and their surface oxides

Since the micron-sized metal and alloy powders are significantly larger compared to the molybdenum oxide powders, they should only be compared in terms of differences in surface oxide composition and relative bioaccessibility in different solutions. The MoO_3 powder, with the largest specific surface area, revealed smaller particle sizes when immersed in PBS compared with dry conditions, most probably due to its dissolution in PBS, *c.f.* Section 3.2. The effect of particle size and particle agglomeration on bioaccessibility testing is discussed in Section 4.3.

To determine whether a Fe(III)/Mo(VI) surface oxide, such as ferrimolybdite, was present on the FeMo powder or not, atomic ratios of oxygen and molybdenum, measured by means of XPS, were compared for the different powders. The atomic ratio was $MoO_{3.1}$ for the MoO_3 powder, $MoO_{2.4}$ for the MoO_2 powder, and $MoO_{2.7}$ for the Mo metal powder. For the FeMo alloy powder, the atomic ratio of oxygen to oxidized molybdenum was 7.2, and 4.4 for the ratio between oxygen and oxidized iron. These ratios are significantly higher compared with corresponding ratios of pure molybdenum- or iron oxides (*e.g.*, MoO_3: 3; MoO_2: 2; Fe_2O_3: 1.5;

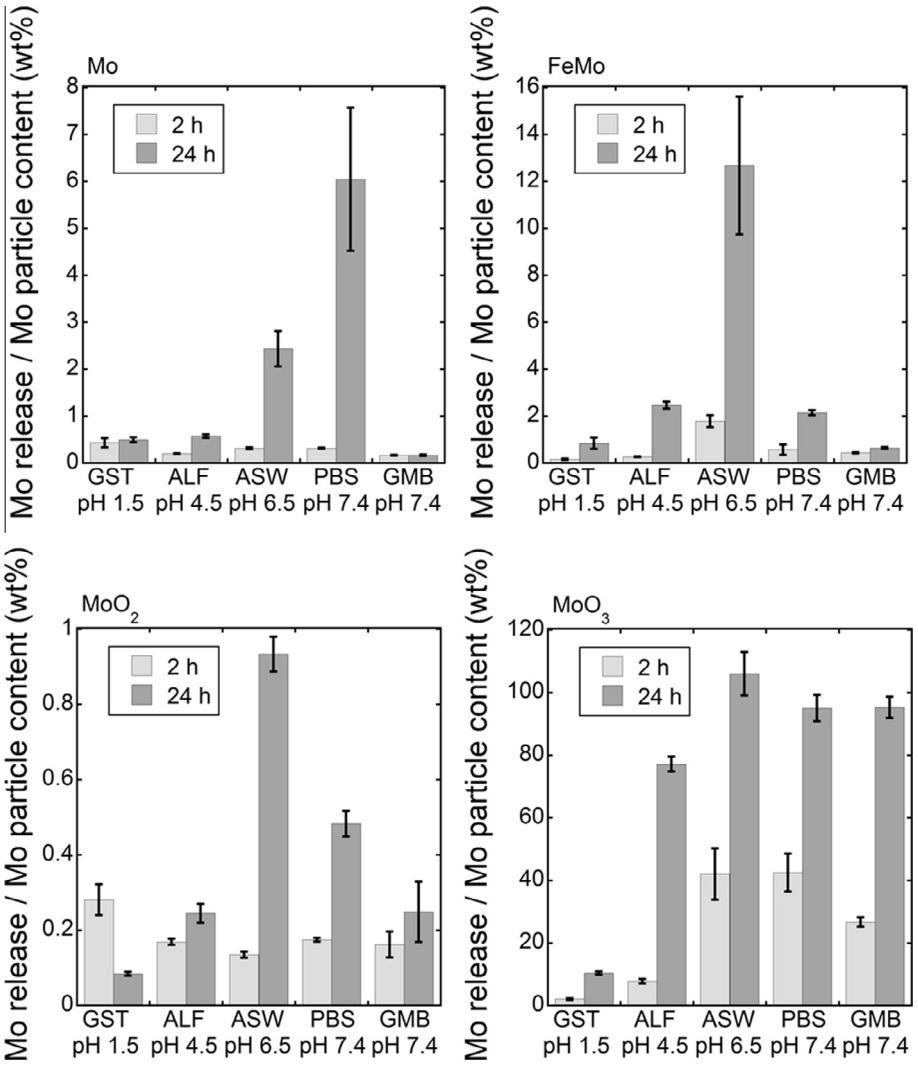

Fig. 2. Released amounts of molybdenum (Mo) normalized to the powder particle content of molybdenum (wt%) for the Mo, FeMo, MoO_2, and MoO_3 powders exposed for 2 and 24 h in different synthetic body fluids (GST – artificial gastric solution; ALF – artificial lysosomal fluid; ASW – artificial sweat; PBS – phosphate buffered saline; GMB – Gamble's solution).

FeOOH: 2) and indicate the presence of another surface oxide constituent, such as ferrimolybdite (atomic ratios: $O/Mo_{(ox)} = 13$; $O/Fe_{(ox)} = 6.5$). There is also a strong indication by means of Raman spectroscopy for a Mo(VI)/Fe(III) phase on the FeMo powder surface, such as ferrimolybdite. Single oxidic phases containing Mo and Fe (*e.g.*, MoO_3, MoO_2, Fe_2O_3, and FeO(OH)) can be excluded, as judged from the Raman spectroscopy results.

To interpret the cyclic voltammetry measurements, available pH-potential diagrams described in the literature were studied. It is according to some reported pH-potential diagrams theoretically possible that there is a solid/solid transformation upon oxidation from Mo(0) or Mo(IV) to Mo(VI) in very acidic environments (Besson and Drautzburg, 1960; Lu and Clayton, 1989; Pardo et al., 2008). This was however discarded already in 1960 in a study that showed direct oxidative dissolution of Mo to Mo(VI) (aq) at acidic conditions (Besson and Drautzburg, 1960). These findings have been confirmed in more recent studies (Presuel-Moreno et al., 2005). Cyclic voltammetry results of this paper could hence not provide any further novel information on the surface oxides of the investigated powders, and the dissolution potentials observed were in agreement with some literature data on electrochemical dissolution of similar metals and oxides (Besson and Drautzburg, 1960).

Concluding the surface oxide characterization, the molybdenum-containing powders tested in this study revealed particle surfaces predominantly composed of Mo(VI)-species, the most oxidized form of molybdenum. A Fe(III)/Mo(VI) oxide was assigned as the main constituent of the surface oxide of the powder particles of the FeMo alloy.

4.2. Metal release in synthetic biological fluids of varying pH and metal complexation capacity

The time periods for exposure in the biological fluids were selected to have some relevance for the inhalation/ingestion scenario. The approximate time for the gastric phase of digestion is about 2 h, and therefore this exposure time period was considered relevant for testing in artificial gastric fluid (Hamel et al., 1998). The 24 h exposure was selected as it can be assumed that human exposure to micron-sized particles lasts no longer than 24 h at ambient conditions. The Mo and FeMo powders showed strongly reduced release rates with time (amount of molybdenum released per time unit), especially in GST (pH 1.5) and GMB (pH 7.4), indicative of improved surface passivity/stabilization over time, or possibly the occurrence of precipitation processes of released molybdenum in solution. Reduced release rates with time were

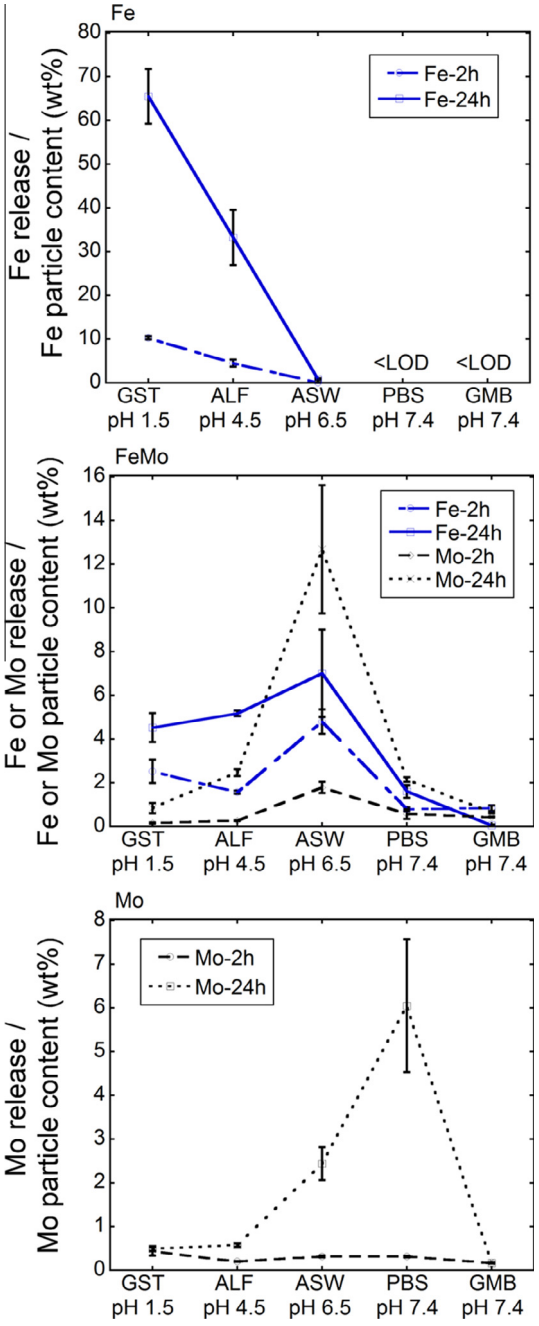

Fig. 3. Release of molybdenum or iron normalized to the corresponding metal particle content (wt%) for the Fe, FeMo, and Mo powders exposed for 2 and 24 h in different synthetic body fluids (GST – artificial gastric solution; ALF – artificial lysosomal fluid; ASW – artificial sweat; PBS – phosphate buffered saline; GMB – Gamble's solution). The lines are only guidance for the eye. <LOD – measured concentrations below the limit of detection. The measured concentration of iron was similar to the limit of detection in the case of released iron from the Fe metal powder after 2 h in ASW.

also observed for the MoO_2 powder, which might be explained by the initial dissolution of less chemically stable particles, or possibly by the precipitation of released molybdenum in GST and/or GMB. However, since no precipitation was observed for molybdenum released from the MoO_3 powder in GST or GMB, precipitation processes are not considered as any main factors that explain the strongly reduced release rates observed for the other powders. Compared with the PBS fluid of similar pH, the chemically complex solution GMB, which contains relatively high amounts of carbonate, has been shown able to passivate metal and metal oxide surfaces and contribute with species that form complexes with released metals in solution that may precipitate (Midander et al., 2010). Low chemical and electrochemical release rates of molybdenum metal and molybdenum oxides are expected at acidic pH (GST, pH 1.5, and ALF, pH 4.5) based on thermodynamic deliberations (Besson and Drautzburg, 1960; Lu and Clayton, 1989; Pardo et al., 2008; Presuel-Moreno et al., 2005) and known chemical dissolution mechanisms of molybdenum oxides (Rollinson, 1975). Relatively higher release rates of molybdenum in ASW (pH 6.5) observed for the FeMo and MoO_2 powders could be related to its higher pH (compared with the GST and ALF solutions) and complexation between lactate and Mo(VI) (Beltrán-Porter et al., 1983).

Bioaccessibility findings of Fe metal, Mo metal, and FeMo alloy powders, Fig. 3, are in agreement with the chemical and electrochemical stability of iron (Pourbaix, 1984) and molybdenum (Besson and Drautzburg, 1960; Lu and Clayton, 1989; Pardo et al., 2008; Presuel-Moreno et al., 2005; Rollinson, 1975), and partly related to the precipitation of released iron in solution at these pH levels (evident from lower measured concentrations of iron in solution after 24 h compared with 2 h of exposure for the FeMo alloy powder, Fig. 3). These processes have previously been described by the authors (Hedberg and Odnevall Wallinder, 2012). Since the surface of the FeMo alloy powder is composed of a Fe(III)/Mo(VI)-oxide, dissolution of the oxide is inhibited in both acidic and alkaline environments, Fig. 3, similar to findings for the Fe/Cr-oxide on stainless steel (Schmuki, 2002; Sedriks, 1996). This explains the relatively high protection against electrochemically and chemically governed release of iron and molybdenum into solution from the FeMo alloy powder in both acidic and neutral/alkaline solutions.

4.3. Influence of powder characteristics and experimental conditions on bioaccessibility

Comparisons between powders of metals, oxides and alloys from a bioaccessibility perspective require that differences in particle and surface characteristics are considered (Hedberg et al., 2013). For powder particles with very similar surface oxide characteristics, a smaller particle size (larger specific surface area) generally results in a larger amount of released metals, and normalization to the surface area is common. However, alloy powders often have surface oxides that are composed of several metals, compositions that vary with the particle size and that depend on the cooling rate and other conditions during particle production (Hedberg et al., 2011a; Hedberg and Midander, 2014). Such differences have for example been shown to result in a significantly higher bioaccessibility (when normalized to the surface area of the particles) for smaller sized stainless steel (AISI 316L) powder particles compared with larger-sized particles of the same alloy in ALF, a solution of high metal complexation capacity (pH 4.5), whereas the opposite situation with higher bioaccessibility was the case for larger compared with smaller sized particles of Fe metal and Cr metal particles (due to particle agglomeration effects in solution) (Hedberg et al., 2010a). The same stainless steel alloy further revealed a lower bioaccessibility for the smaller-sized powder compared with the larger-sized powder (when normalized to the surface area) in non-complexing or neutral solutions such as PBS (Hedberg et al., 2013). This behavior is explained by their surface oxide characteristics with certain susceptibilities to complexation-induced chemical dissolution or electrochemical corrosion (Hedberg and Midander, 2014).

Besides the particle size that influences the surface oxide characteristics, at least for alloy powders, the extent of agglomeration in solution during bioaccessibility testing largely influences the results. The degree of agglomeration depends on the powder characteristics, primarily its isoelectric point, and on the solution

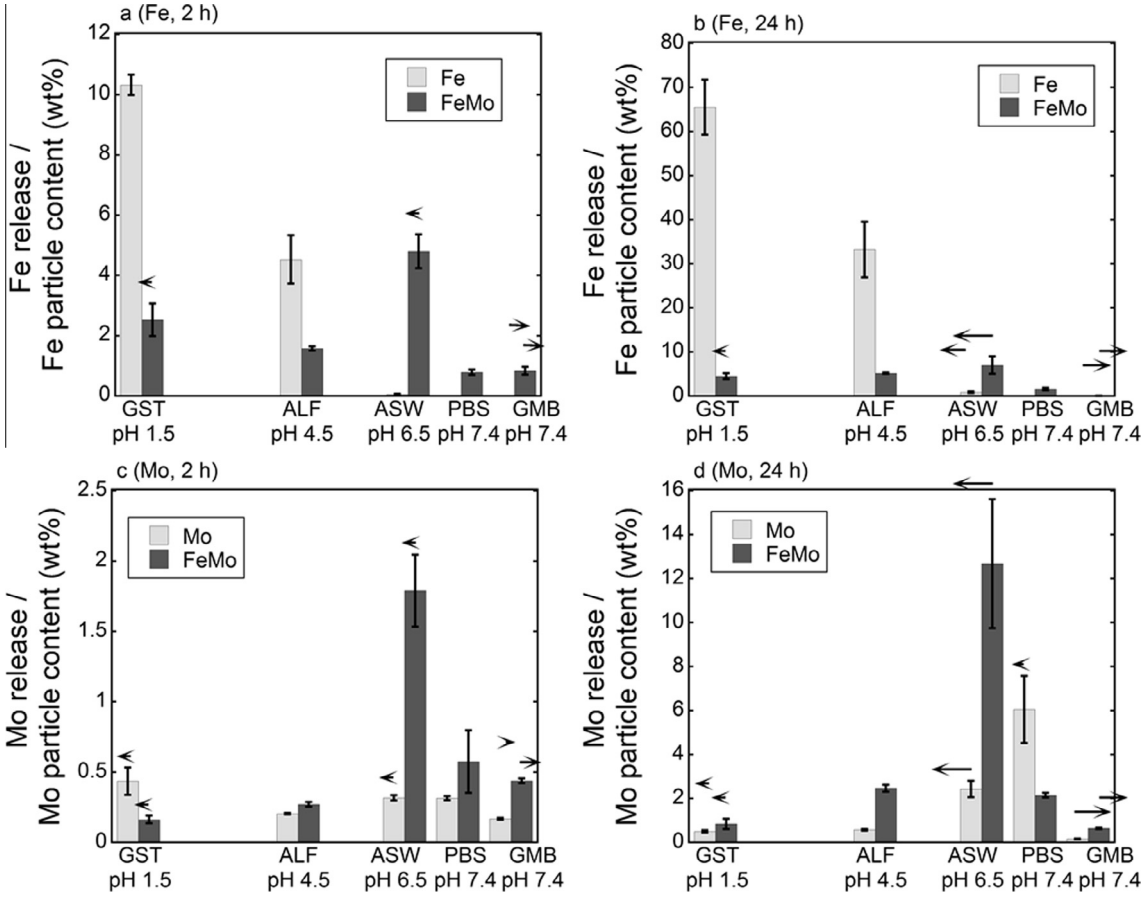

Fig. 4. Release of molybdenum or iron normalized to the corresponding metal particle content (wt%) for the Fe (a–b), FeMo (a–d), and Mo (c–d) powders exposed for 2 (a and c) and 24 h (b and d) in different synthetic body fluids of varying pH (pH 1.5, GST – artificial gastric solution; pH 4.5, ALF – artificial lysosomal fluid; pH 6.5, ASW – artificial sweat; pH 7.4, PBS – phosphate buffered saline; pH 7.4, GMB – Gamble's solution). The arrows indicate changes of the pH during exposure. The measured concentration of iron released from the Fe metal powder was similar to the limit of detection after 2 h in artificial sweat, and below the limit of detection in phosphate buffered saline and Gamble's solution.

characteristics in terms of pH and ionic strength, characteristics that influence attractive forces between particles (van Oss, 2006). In this study, the highest extent of agglomeration was observed for the MoO_2 powder. The degree of particle agglomeration in solution was dissimilar among the different investigated powders.

Agglomeration is further influenced by the loading (powder mass per solution volume), and sample preparation such as sonication of particle dispersions (Cronholm et al., 2011; Hedberg et al., 2010a; Karlsson et al., 2013; Midander et al., 2006). The loading affects further the chemical equilibrium between dissolved and solid species, suppressing metal release at very high loadings. Thus, these effects need to be considered in solubility studies.

Only relative comparisons between the powders are hence possible in this study due to their differences in specific surface areas and extent of agglomeration in solution, which results in different amounts of released molybdenum into solution per particle mass.

4.4. Implications for risk assessments of alloys

The strong non-linear influence of particle characteristics, experimental conditions, and surface oxide characteristics of metal or alloy powder on the extent of released metals into solution mean that the bioaccessibility of a given metallic powder can vary significantly, depending on specific bulk and surface properties, and experimental conditions would benefit from standardization.

Prevailing experimental conditions, particle- and surface oxide characteristics also influence the rate of particle dissolution. The rate of dissolution of pharmaceuticals or salts is often described by the Noyes Whitney equation, which correlates to e.g. the surface area of the interface between the dissolving substance and the solvent, and to the diffusion coefficient (Dokoumetzidis and Macheras, 2006). However, this description is not applicable to particles of passive metals and alloys as they have surface oxides of different composition than in the bulk alloy, and that hinder diffusion processes at room or body temperatures (Rapp, 1984). Instead, metal release processes from powder particles of metals and alloys in solution are predominantly the result of surface defects, complexation-induced dissolution, and/or metastable corrosion processes (Hedberg et al., 2012; Hedberg and Midander, 2014).

Alloy bioaccessibility (metal release) is, in the case of lack of data, sometimes estimated from existing data on their pure metal constituents, if available (EC, 2007). This approach has been shown erroneous for alloys such as stainless steels, ferrochromium alloys, and ferrosilicochromium alloys (Hedberg et al., 2013; Herting et al., 2005; Hillwalker and Anderson, 2014; Midander et al., 2010; Santonen et al., 2010; Stockmann-Juvala et al., 2013). A main reason is that these alloys all have surface oxides that have different properties compared with surface oxides of their individual metal constituents, and that all alloy components may not be present in the outermost surface oxide but may appear in adjacent alloy surface layers beneath the oxide, or in the bulk alloy. Such alloys reveal, compared with their pure alloy constituents, relatively higher corrosion resistances in similar synthetic body fluids as

Table 5
Average difference in iron released per iron content in the powder (wt%), and molybdenum released per molybdenum content in the powder (wt%), after 2 and 24 h of exposure in the different synthetic body fluids. Corresponding average difference presented as metal released per particle surface area (based on the specific surface area measured by the BET method), in $\mu g/cm^2$, is given in parentheses.

pH and fluid	2 h: Mo difference FeMo–Mo powders	24 h: Mo difference FeMo–Mo powders	2 h: Fe difference FeMo–Fe powders	24 h: Fe difference FeMo–Fe powders
1.5 (GST)	−0.28 (+5.0)	+0.35 (+10)	−7.8 (−315)	−61 (−2030)
4.5 (ALF)	+0.06 (+3.4)	+1.9 (+12)	−2.9 (−136)	−28 (−1008)
6.5 (ASW)	+1.5 (+12)	+10 (+8.5)	+4.7 (+23)	+6.2 (+74)
7.4 (PBS)	+0.26 (+0.8)	−3.9 (−22)	+0.79 (+5.8)	+1.6 (+18)
7.4 (GMB)	+0.27 (+1.6)	+0.5 (−0.6)	+0.84 (+5.1)	+0.05 (+4.3)

GST – artificial gastric solution; ALF – artificial lysosomal fluid; ASW – artificial sweat; PBS – phosphate buffered saline; GMB – Gamble's solution.

examined in this study, and also lower amounts of released metals into solution. For example, less than 0.3% of the particle mass of powders of stainless steel, ferrochromium alloys, and ferrosilicochromium alloys, compared with less than 100% for iron and nickel metal powders, was released into solution when exposed to the same biological fluids as investigated in this study (Hedberg et al., 2010b; Midander et al., 2010). In this study less than 12% of the particle mass of the FeMo alloy powder was released at similar conditions.

A comparison of released amounts of metals normalized by the corresponding metal content of each powder, or to the specific surface area of the powder particles, is compiled for the Fe, Mo, and FeMo powders of this study in Figs. 3 and 4 and Table 5. Assuming that the FeMo alloy (30.2 wt% Fe, 69.8 wt% Mo) would behave as a mixture of its pure metal constituents, the estimated release of iron and molybdenum (based on 24 h exposure data in wt%) would become highly erroneous and deviate significantly from the measured bioaccessibility. The release of iron from the FeMo alloy powder would be highly overestimated in acidic solutions (15-fold in GST, 6-fold in ALF) when compared to the Fe metal powder, whereas the release of molybdenum would be underestimated at similar conditions (2-fold in GST, 4-fold in ALF), Fig. 4. In neutral and alkaline solutions, the release of iron would be highly underestimated (8-fold in ASW, unlimited in PBS and GMB), and the release of molybdenum under- or overestimated (5-fold underestimated in ASW, 3-fold overestimated in PBS, and 4-fold underestimated in GMB). This comparison clearly illustrates that the Fe(III)/Mo(VI) surface oxide at the FeMo alloy particle surface hinders the release of iron at acidic conditions, and possibly of molybdenum at alkaline pH, but not in ASW (pH 6.5), despite the fact that the overall release was not significantly lower from the FeMo powder compared with the powders of its pure metal constituents. This is caused by the ability of such oxides on alloys to adjust their outermost oxide composition to the environment (Hedberg et al., 2013; Virtanen et al., 2008). This example hence demonstrates that alloys do not behave as their pure metal constituents, even if the alloy has a relatively low corrosion resistance or exhibits similar extents of total metal release compared with its pure metal constituents.

5. Conclusions

This study links particle characteristics and surface composition of powder particles of Mo metal, Fe metal, a FeMo alloy, and oxides of MoO_2 and MoO_3 with quantitative data after 2 and 24 h of exposure to the release of molybdenum and iron in five synthetic body fluids of varying pH and metal complexation capacity relevant for different human exposure routes including dermal contact, inhalation and ingestion. The following main conclusions were drawn:

1. A Fe(III)/Mo(VI) oxide at the particle surface of the FeMo alloy powder hindered the release of iron at acidic conditions and possibly of molybdenum at weakly alkaline conditions, but not at near neutral conditions (artificial sweat). Despite a total amount of released metals in the same order of magnitude compared with its pure alloy components, the released amount of iron and molybdenum from the FeMo powder would be strongly over- or underestimated if predicted from metal release data of the pure elements, when exposed at similar conditions.
2. Bioaccessibility of the FeMo alloy powder cannot be predicted based on data from powder particles of its pure alloying elements.
3. More molybdenum was released at higher pH from powder particles of Mo metal and of oxides of MoO_2 and MoO_3. The weakly alkaline Gamble's solution (GMB, pH 7.4), which contains a significant amount of carbonates, most probably induced surface passivation for most powders and/or precipitation of molybdenum from solution, and thereby significantly lower amounts of released molybdenum compared with observations in the weakly alkaline PBS solution of similar pH.
4. The Mo powder released lower amounts of molybdenum after 24 h compared with 2 h due to surface passivation/stabilization, processes that were mostly pronounced in the acidic gastric solution GST (pH 1.5) and in GMB (pH 7.4).
5. Molybdenum was released from the Mo powder up to 6% in PBS, up to 2% in ASW and less than 1% in GST, ALF and GMB. For the FeMo powder, molybdenum was released up to 13% in artificial sweat (ASW, pH 6.5), about 2% in PBS and ALF, and less than 1% in GMB and GST.

Conflict of Interest

The authors declare that they have no conflict interest.

Transparency Document

The Transparency document associated with this article can be found in the online version.

Acknowledgments

The International Molybdenum Association (IMOA), Iron Consortium (Iron Platform Services Ltd), KTH faculty grants, and the Swedish Research Council (VR, Grant number 2013-5621) are acknowledged for their financial support. Dr. Kevin Klipsch, EBRC Consulting GmbH, Germany, and Dr. Philip Mitchell, University of Reading, UK, are highly acknowledged for scientific discussions. Dr. Jonas Hedberg, KTH, is gratefully acknowledged for assistance in the Raman measurements and help in their analytical evaluation.

References

Anthony, J.W., Bideaux, R.A., Bladh, K.W., Nichols, M.C., 1990. Handbook of Mineralogy. Mineral Data Publishing, Tucson Arizona, USA.

Anwar, M., Hogarth, C., Bulpett, R., 1989. Effect of substrate temperature and film thickness on the surface structure of some thin amorphous films of MoO_3 studied by X-ray photoelectron spectroscopy (ESCA). J. Mater. Sci. 24, 3087–3090.

Beltrán-Porter, A., Cervilla, A., Caturla, F., Vila, M.J., 1983. Lactate complexes of molybdenum (VI). Transit. Met. Chem. 8, 324–328.

Besson, J., Drautzburg, G., 1960. Das anodische Verhalten der Metalle Molybdän und Wolfram. Electrochim. Acta 3, 158–168.

Brunauer, S., Emmet, P.H., Teller, E., 1938. Adsorption of gases in multimolecular layers. J. Am. Chem. Soc. 60, 309–319.

CEN, 2011. Reference Test Method for Release of Nickel from all Post Assemblies Which are Inserted into Pierced Parts of the Human Body and Articles Intended to Come into Direct and Prolonged Contact With the Skin, EN-1811:2011.

Chan, W.Y., Clendenning, S.B., Berenbaum, A., Lough, A.J., Aouba, S., Ruda, H.E., Manners, I., 2005. Highly metallized polymers: synthesis, characterization, and lithographic patterning of polyferrocenylsilanes with pendant cobalt, molybdenum, and nickel cluster substituents. J. Am. Chem. Soc. 127, 1765–1772.

Cobb, A., Schmalzreid, T., 2006. The clinical significance of metal ion release from cobalt-chromium metal-on-metal hip joint arthroplasty. Proc. Inst. Mech. Eng. [H] 220, 385–398.

Colton, R.J., Guzman, A.M., Rabalais, J.W., 1978. Electrochromism in some thin-film transition-metal oxides characterized by X-ray electron spectroscopy. J. Appl. Phys. 49, 409–416.

Cronholm, P., Midander, K., Karlsson, H.L., Elihn, K., Odnevall Wallinder, I., Möller, L., 2011. Effect of sonication and serum proteins on copper release from copper nanoparticles and the toxicity towards lung epithelial cells. Nanotoxicology 5, 269–281.

de Meringo, A., Morscheidt, C., Thélohan, S., Tiesler, H., 1994. In vitro assessment of biodurability: acellular systems. Environ. Health Perspect. 102, 1–6.

Dokoumetzidis, A., Macheras, P., 2006. A century of dissolution research: from Noyes and Whitney to the biopharmaceutics classification system. Int. J. Pharm. 321, 1–11.

EC, 2009. Glossary, CLP Regulation, No 1272/2008. <http://ec.europa.eu/enterprise/sectors/chemicals/files/ghs/ghs_sc_glossary_en.pdf/> (accessed 10.05.15).

EC, 2007. REACH – Registration, Evaluation, Authorisation and Restriction of Chemicals. European Commission Environment Directorate General. <http://ec.europa.eu/enterprise/sectors/chemicals/reach/index_en.htm/> (accessed 10.05.15).

Fleischer, M., Pabst, A., 1981. New mineral names. Am. Mineral. 66, 436–439.

Fujii, T., De Groot, F., Sawatzky, G., Voogt, F., Hibma, T., Okada, K., 1999. In situ XPS analysis of various iron oxide films grown by NO_2-assisted molecular-beam epitaxy. Phys. Rev. B. 59, 3195.

Grosvenor, A., Kobe, B., Biesinger, M., McIntyre, N., 2004. Investigation of multiplet splitting of Fe 2p XPS spectra and bonding in iron compounds. Surf. Interface Anal. 36, 1564–1574.

Hamel, S.C., Buckley, B., Lioy, P.J., 1998. Bioaccessibility if metals in soils for different liquid to solid ratios in synthetic gastric fluid. Environ. Sci. Technol. 32, 358–362.

Hanawa, T., 2004. Metal ion release from metal implants. Mater. Sci. Eng., C 24, 745–752.

Hedberg, Y., Midander, K., 2014. Size matters: mechanism of metal release from 316L stainless steel particles is governed by size-dependent properties of the surface oxide. Mater. Lett. 122, 223–226.

Hedberg, Y., Odnevall Wallinder, I., 2012. Transformation/dissolution studies on the release of iron and chromium from particles of alloys compared with their pure metals and selected metal oxides. Mater. Corros. 63, 481–491.

Hedberg, Y., Odnevall Wallinder, I., 2014. Metal release and speciation of released chromium from a biomedical CoCrMo alloy into simulated physiologically relevant solutions. J. Biomed. Mater. Res. B 102, 693–699.

Hedberg, Y., Gustafsson, J., Karlsson, H.L., Möller, L., Odnevall Wallinder, I., 2010a. Bioaccessibility, bioavailability and toxicity of commercially relevant iron- and chromium-based particles: in vitro studies with an inhalation perspective. Part. Fibre Toxicol. 7, 23.

Hedberg, Y., Midander, K., Odnevall Wallinder, I., 2010b. Particles, sweat, and tears: a comparative study on bioaccessibility of ferrochromium alloy and stainless steel particles, the pure metals and their metal oxides, in simulated skin and eye contact. Integr. Environ. Assess. Manag. 6, 456–468.

Hedberg, Y., Karlsson, O., Szakalos, P., Odnevall Wallinder, I., 2011a. Ultrafine 316 L stainless steel particles with frozen-in magnetic structures characterized by means of electron backscattered diffraction. Mater. Lett. 65, 2089–2092.

Hedberg, Y., Hedberg, J., Liu, Y., Odnevall Wallinder, I., 2011b. Complexation- and ligand-induced metal release from 316L particles: importance of particle size and crystallographic structure. Biometals 24, 1099–1114.

Hedberg, Y., Norell, M., Linhardt, P., Bergqvist, H., Odnevall Wallinder, I., 2012. Influence of surface oxide characteristics and speciation on corrosion, electrochemical properties and metal release of atomized 316L stainless steel powders. Int. J. Electrochem. Sci. 7, 11655–11677.

Hedberg, Y., Mazinanian, N., Odnevall Wallinder, I., 2013. Metal release from stainless steel powders and massive sheet – comparison and implication for risk assessment of alloys. Environ. Sci. Process. Impacts 15, 381–392.

Hedberg, Y., Qian, B., Zhijian, S., Virtanen, S., Odnevall Wallinder, I., 2014. In-vitro biocompatibility of CoCrMo dental alloys fabricated by selective laser melting. Dent. Mater. 30, 525–534.

Herting, G., Odnevall Wallinder, I., Leygraf, C., 2005. A comparison of release rates of Cr, Ni, and Fe from stainless steel alloys and the pure metals exposed to simulated rain events. J. Electrochem. Soc. 152, B23–B29.

Hillwalker, W.E., Anderson, K.A., 2014. Bioaccessibility of metals in alloys: evaluation of three surrogate biofluids. Environ. Pollut. 185, 52–58.

Hodgson, A.W.E., Kurz, S., Virtanen, S., Fervel, V., Olsson, C.O.A., Mischler, S., 2004. Passive and transpassive behaviour of CoCrMo in simulated biological solutions. Electrochim. Acta 49, 2167–2178.

Ichinose, S., Muneta, T., Sekiya, I., Itoh, S., Aoki, H., Tagami, M., 2003. The study of metal ion release and cytotoxicity in Co–Cr–Mo and Ti–Al–V alloy in total knee prosthesis – scanning electron microscopic observation. J. Mater. Sci. - Mater. Med. 14, 79–86.

Karimi, S., Nickchi, T., Alfantazi, A.M., 2012. Long-term corrosion investigation of AISI 316L, Co–28Cr–6Mo, and Ti–6Al–4V alloys in simulated body solutions. Appl. Surf. Sci. 258, 6087–6096.

Karlsson, H.L., Cronholm, P., Hedberg, Y., Tornberg, M., Battice, L., Svedhem, S., Odnevall Wallinder, I., 2013. Cell membrane damage and protein interaction of copper containing nanoparticles: surface- and metal release dependent effects. Toxicology 313, 59–69.

Kerr, P., Langer, A., Thomas, A., 1963. Nature and synthesis of ferrimolybdite. Am. Mineral. 48, 14–32.

Kihlborg, L., 1963. Least squares refinement of crystal structure of molybdenum trioxide. Arkiv for Kemi 21, 357–364.

Kocijan, A., Milošev, I., Pihlar, B., 2004. Cobalt-based alloys for orthopaedic applications studied by electrochemical and XPS analysis. J. Mater. Sci. - Mater. Med. 15, 643–650.

Kruglova, V.G., Poteryaikina, A.A., Sidorenko, G.A., Dubakina, L.S., Ryabeva, E.G., 1980. Tugarinovite, (MoO_2), a new hypogene molybdenum mineral. Zap. Vses. Mineral. O-va. 109, 465–468.

Kumari, L., Ma, Y.-R., Tsai, C.-C., Lin, Y.-W., Wu, S.Y., Cheng, K.-W., Liou, Y., 2007. X-ray diffraction and Raman scattering studies on large-area array and nanobranched structure of 1D MoO_2 nanorods. Nanotechnology 18, 115717.

Lee, S.-H., Deshpande, R., Benhammou, D., Parilla, P.A., Mahan, A., Dillon, A.C., 2009. Metal oxide nanoparticles for advanced energy applications. Thin Solid Films 517, 3591–3595.

Lewis, A.C., Kilburn, M.R., Papageorgiou, I., Allen, G.C., Case, C.P., 2005. Effect of synovial fluid, phosphate-buffered saline solution, and water on the dissolution and corrosion properties of CoCrMo alloys as used in orthopedic implants. J. Biomed. Mater. Res. A 73A, 456–467.

Linhardt, P., 1998. Electrochemical identification of higher oxides of manganese in corrosion relevant deposits formed by microorganisms. Mater. Sci. Forum 289, 1267–1274.

Lu, Y.C., Clayton, C.R., 1989. An XPS study of the passive and transpassive behavior of molybdenum in deaerated 0.1 M HCl. Corros. Sci. 29, 927–937.

Mazinanian, N., Odnevall Wallinder, I., Hedberg, Y., 2015. Comparison of the influence of citric acid and acetic acid as simulant for acidic food on the release of alloy constituents from stainless steel AISI 201. J. Food Eng. 145, 51–63.

Mestl, G., Ruiz, P., Delmon, B., Knozinger, H., 1994. Oxygen-exchange properties of MoO_3: an in situ Raman spectroscopy study. J. Phys. Chem. 98, 11269–11275.

Metikoš-Huković, M., Pilić, Z., Babić, R., Omanović, D., 2006. Influence of alloying elements on the corrosion stability of CoCrMo implant alloy in Hank's solution. Acta Biomater. 2, 693–700.

Midander, K., Pan, J., Leygraf, C., 2006. Elaboration of a test method for the study of metal release from stainless steel particles in artificial biological media. Corros. Sci. 48, 2855–2866.

Midander, K., de Frutos, A., Hedberg, Y., Darrie, G., Odnevall Wallinder, I., 2010. Bioaccessibility studies of ferro-chromium alloy particles for a simulated inhalation scenario: a comparative study with the pure metals and stainless steel. Integr. Environ. Assess. Manag. 6, 441–455.

Neugebauer, H., Nauer, G., Brinda-Konopik, N., Gidaly, G., 1981. The in situ determination of oxidation products on iron electrodes in alkaline electrolytes using multiple internal reflection Fourier transform infrared spectroscopy. J. Electroanal. Chem. Interface Electrochem. 122, 381–385.

OECD CoCAM programme, 2013. SIDS initial assessment profile for highly soluble molybdenum salts, pdf available on: <http://webnet.oecd.org/HPV/UI/handler.axd?id=7feeff59-de60-4000-8d08-f3c9c7770149/> (accessed 10.05.15).

Okazaki, Y., Gotoh, E., 2005. Comparison of metal release from various metallic biomaterials in vitro. Biomaterials 26, 11–21.

Okazaki, Y., Gotoh, E., 2008. Metal release from stainless steel, Co–Cr–Mo–Ni–Fe and Ni–Ti alloys in vascular implants. Corros. Sci. 50, 3429–3438.

Öztürk, O., Türkan, U., Eroglu, A.E., 2006. Metal ion release from nitrogen ion implanted CoCrMo orthopedic implant material. Surf. Coat. Technol. 200, 5687–5697.

Pardo, A., Merino, M.C., Coy, A.E., Viejo, F., Arrabal, R., Matykina, E., 2008. Pitting corrosion behaviour of austenitic stainless steels – combining effects of Mn and Mo additions. Corros. Sci. 50, 1796–1806.

Pourbaix, M., 1984. Electrochemical corrosion of metallic biomaterials. Biomaterials 5, 122–134.

Presuel-Moreno, F., Jakab, M., Scully, J., 2005. Inhibition of the oxygen reduction reaction on copper with cobalt, cerium, and molybdate ions. J. Electrochem. Soc. 152, B376–B387.
Rapp, R.A., 1984. The high temperature oxidation of metals forming cation-diffusing scales. Metall. Mater. Trans. B 15, 765–782.
Rollinson, C.L., 1975. The Chemistry of Chromium, Molybdenum, and Tungsten. Robert Maxwell M.C., Oxford, UK.
Santonen, T., Stockmann-Juvala, H., Zitting, A., 2010. Review on Toxicity of Stainless Steel, ISBN 978-952-261-039-3. Finnish Institute of Occupational Health, Helsinki, Finland.
Schmuki, P., 2002. From Bacon to barriers: a review on the passivity of metals and alloys. J. Solid State Electrochem. 6, 145–164.
Sedriks, A.J., 1996. Corrosion of Stainless Steels. John Wiley & Sons Inc, New York.
Sejkora, J., Čejka, J., Malíková, R., López, A., Xi, Y., Frost, R.L., 2014. A Raman spectroscopic study of a hydrated molybdate mineral ferrimolybdite, $Fe_2(MoO_4)_3$ 7–8H_2O. Spectrochim. Acta A 130, 83–89.
Sengupta, J., Ghosh, S., Datta, P., Gomes, A., Gomes, A., 2014. Physiologically important metal nanoparticles and their toxicity. J. Nanosci. Nanotechnol. 14, 990–1006.
Solferino, G., Anderson, A.J., 2012. Thermal reduction of molybdite and hematite in water and hydrogen peroxide-bearing solutions: Insights on redox conditions in Hydrothermal Diamond Anvil Cell (HDAC) experiments. Chem. Geol. 322, 215–222.
Stockmann-Juvala, H., Hedberg, Y., Dhinsa, N.K., Griffiths, D.R., Brooks, P.N., Zitting, A., Odnevall Wallinder, I., Santonen, T., 2013. Inhalation toxicity of 316L stainless steel powder in relation to bioaccessibility. Hum. Exp. Toxicol. 32, 1137–1154.
Stopford, W., Turner, J., Cappellini, D., Brocka, T., 2003. Bioaccessibility testing of cobalt compounds. J. Environ. Monit. 5, 675–680.
van Oss, C.J., 2006. Interfacial Forces in Aqueous Media. Taylor & Francis Group, LLC, Boca Raton.
Virtanen, S., Milosev, I., Gomez-Barrena, E., Trebse, R., Salo, J., Konttinen, Y.T., 2008. Special modes of corrosion under physiological and simulated physiological conditions. Acta Biomater. 4, 468.
Wataha, J.C., 2000. Biocompatibility of dental casting alloys: a review. J. Prosthet. Dent. 83, 223–234.
Werfel, F., Minni, E., 1983. Photoemission study of the electronic structure of Mo and Mo oxides. J. Phys. Chem. C Solid State 16, 6091.